An Experimental and Theoretical Investigation of the Chemical Shielding Tensors of $^{13}C^{\alpha}$ of Alanine, Valine, and Leucine Residues in Solid Peptides and in Proteins in Solution

Robert H. Havlin,[†,‡] David D. Laws,[†,‡] Hans-Marcus L. Bitter,[†,‡] Lori K. Sanders,[||] Haihong Sun,[⊥] Joshua S. Grimley,[||] David E. Wemmer,[†,§] Alexander Pines,[†,‡] and Eric Oldfield*[,||,⊥]

Contribution from the Department of Chemistry, University of California, Berkeley, California 94720, Materials Sciences and Physical Biosciences Divisions, Lawrence Berkeley National Laboratory, 1 Cyclotron Road, Berkeley, California 94720, and Departments of Chemistry and Biophysics, University of Illinois at Urbana-Champaign, 600 South Mathews Avenue, Urbana Illinois, 61801

Received June 20, 2001. Revised Manuscript Received August 13, 2001

Abstract: We have carried out a solid-state magic-angle sample-spinning (MAS) nuclear magnetic resonance (NMR) spectroscopic investigation of the $^{13}C^{\alpha}$ chemical shielding tensors of alanine, valine, and leucine residues in a series of crystalline peptides of known structure. For alanine and leucine, which are not branched at the β-carbon, the experimental chemical shift anisotropy (CSA) spans (Ω) are large, about 30 ppm, independent of whether the residues adopt helical or sheet geometries, and are in generally good accord with Ω values calculated by using ab initio Hartree−Fock quantum chemical methods. The experimental Ωs for valine C^{α} in two peptides (in sheet geometries) are also large and in good agreement with theoretical predictions. In contrast, the "CSAs" ($\Delta\sigma^*$) obtained from *solution* NMR data for alanine, valine, and leucine residues in proteins show major differences, with helical residues having $\Delta\sigma^*$ values of ∼6 ppm while sheet residues have $\Delta\sigma^* \approx 27$ ppm. The origins of these differences are shown to be due to the different definitions of the CSA. When defined in terms of the solution NMR CSA, the solid-state results also show small helical but large sheet CSA values. These results are of interest since they lead to the idea that only the β-branched amino acids threonine, valine, and isoleucine can have small (static) tensor spans, Ω (in helical geometries), and that the small helical "CSAs" seen in solution NMR are overwhelmingly dominated by changes in tensor *orientation*, from sheet to helix. These results have important implications for solid-state NMR structural studies which utilize the CSA span, Ω, to differentiate between helical and sheet residues. Specifically, there will be only a small degree of spectral editing possible in solid proteins since the spans, Ω, for the dominant nonbranched amino acids are quite similar. Editing on the basis of Ω will, however, be very effective for many Thr, Val, and Ileu residues, which frequently have small (∼15−20 ppm) helical CSA (Ω) spans.

Introduction

Over the past few years, there has been an increased interest in the use of the isotropic chemical shift and the chemical shift (or shielding) tensor in investigating peptide and protein structure. This work has included a number of ab initio and density functional theory quantum chemical investigations aimed at relating chemical shifts and shift anisotropies to structure.[1−6] In early work, Spera and Bax[7] reported clear differences between isotropic C^{α} and C^{β} shifts in helical and sheet geometries, and these shifts have been quite accurately predicted by using quantum chemical methods.[8] Recently, we have reported experimental and theoretical shift (or shielding) tensor results, σ_{ii}, for a series of alanine-containing peptides.[9] We also demonstrated that peptide backbone ϕ,ψ angles could be derived from the experimental shift tensor results, using a Bayesian probability method.[9] In addition, we also reported the results of a theoretical study of the C^{α} shielding tensors in Gly, Ala, Val, Ser, Thr, and Ileu containing peptide fragments.[10] We noted that for C^{β}-substituted amino acids (valine, isoleucine, serine, and threonine) not only was the ∼4−5 ppm increase in isotropic shielding of sheet conformations over helical ones observed, but in general there was also a large increase in overall tensor span ($\Omega = \sigma_{33} - \sigma_{11}$), and a change in tensor orientation, for sheet versus helical residues.[10] More recently, this difference in tensor span has been used in the identification of protein secondary structure in the solid state using a CSA-based spectral editing technique.[11]

[†] Department of Chemistry, University of California.
[‡] Materials Sciences Division, Lawrence Berkeley National Laboratory.
[§] Physical Biosciences Division, Lawrence Berkeley National Laboratory.
[||] Department of Chemistry, University of Illinois at Urbana-Champaign.
[⊥] Department of Biophysics, University of Illinois at Urbana-Champaign.

(1) Le, H.; Pearson, J. G.; de Dios A. C.; Oldfield, E. *J. Am. Chem. Soc.* **1995,** *117,* 3800−3807.
(2) Pearson, J. G.; Wang, J.-F.; Markley, J. L.; Le, H.; Oldfield, E. *J. Am. Chem. Soc.* **1995**, *117*, 8823−8829.
(3) Oldfield, E. *J. Biomol. NMR* **1995**, *5*, 217−225.
(4) Sitkoff, D.; Case, D. A. *Prog. Nucl. Magn. Reson. Spectrosc.* **1998**, *32*, 165−190.
(5) Case, D. A. *Curr. Opin. Struct. Biol.* **1998**, *8*, 624−630.
(6) Case, D. A. *Curr. Opin. Struct. Biol.* **2000**, *10*, 197−203.
(7) Spera, S.; Bax. A. *J. Am. Chem. Soc.* **1991**, *113*, 5490−5492.
(8) de Dios, A. C.; Pearson J. G.; Oldfield, E. *Science* **1993**, *260*, 1491−1496.
(9) Heller, J.; Laws, D. D.; King, D. S.; Wemmer, D. E.; Pines, A.; Havlin R. H.; Oldfield, E. *J. Am. Chem. Soc.* **1997**, *119*, 7827−7831.
(10) Havlin, R. H.; Le, H.; Laws, D. D.; deDios A. C.; Oldfield, E. *J. Am. Chem. Soc.* **1997**, *119*, 11951−11958.

10.1021/ja0115060 CCC: $20.00
Published on Web 09/28/2001

In solution NMR cross-correlation measurements, Tjandra and Bax[12] also obtained quantitative experimental information on the $^{13}C^{\alpha}$ CSA which correlated with backbone structure: on average in α-helices, $\sigma_{orth} - \sigma_{par} = 6.1 \pm 4.9$ ppm whereas in β-sheets, $\sigma_{orth} - \sigma_{par} = 27.1 \pm 4.3$ ppm, where σ_{par} is the shielding in the direction parallel to the C−H bond and σ_{orth} is the average shielding orthogonal to this bond. This effect was first predicted theoretically by Walling et al.,[13] who investigated "idealized" helical ($\phi = -60°$, $\psi = -60°$) and sheet ($\phi = -120°$, $\psi = 120°$) geometries for 18 amino acids, and Sitkoff and Case[4] then made a direct comparison of the $^{13}C^{\alpha}$ CSA values for ubiquitin and calmodulin/M13 using an alanine fragment,[4] and we made similar correlations for several other amino acids.[14]

There are, however, a number of apparently puzzling observations. First of all, Sitkoff and Case[4] were able to reproduce reasonably well the entire set of reported ubiquitin and calmodulin CSA values ($\Delta\sigma^* = \sigma_{orth} - \sigma_{par}$) just by using alanine as a model for all amino acids, but alanine is known to have about the same CSA, Ω, in both helical and sheet geometries.[10] This suggests that the "CSAs" measured in solution are overwhelmingly dominated by a change in shift tensor orientation, as first suggested by Walling et al.,[13] not by any change in the span (Ω) seen in solid-state NMR, or from $\Omega = \sigma_{33} - \sigma_{11} = \Delta\sigma$ values obtained from calculation. Second, in recent unpublished calculations on phenylalanine, tyrosine, leucine, cysteine, and lysine,[15] we have found that C^{α} spans are essentially the *same* in both helical and sheet residues: only C^{α} of threonine, valine, and isoleucine appear to show large differences in CSA (Ω) between helical (Ω ≈ 20 ppm) and sheet (Ω ≈ 34 ppm) geometries.[10,15] In previous work, we included serine as a member of a substituted amino acid class (Val, Ileu, Thr, and Ser), but the results of our more recent work suggest that a more (NMR) appropriate classification of the amino acids is β-branched (two substitions on C^{β}, i.e., Val, Thr, and Ileu) and nonbranched (the remaining amino acids). If correct, this would have important implications for spectral editing experiments based on Ω or for structural conclusions which might be drawn from Ω . We have therefore carried out an experimental and theoretical investigation of the $^{13}C^{\alpha}$ shielding tensors in two nonbranched amino acids, alanine and leucine, in a series of crystalline peptides, in addition to investigating C^{α} shielding in valine in small peptides, to validate the results of the quantum chemical calculations on small molecules. The results confirm the theoretical predictions. In addition, we have carried out a theoretical investigation of the $^{13}C^{\alpha}$ $\Delta\sigma^* = \sigma_{orth} - \sigma_{par}$ values of these and other peptides in the solid state. The results for leucine are particularly interesting since they show that both helical and sheet fragments have the same CSA (Ω), because leucine is an unbranched amino acid, but due to tensor rotations, $\Delta\sigma^* = \sigma_{orth} - \sigma_{par}$ for solid leucine residues range from ∼10 to 30 ppm, just as those found in solution NMR investigations.

Experimental Section

Synthetic Aspects. Four peptides were synthesized: LL*VY-OMe,[16] L*LVY-OMe, Boc-V*AL-Aib-*VAL-OMe, and Boc-VA*L-Aib-VAL-OMe. An "*" placed before an amino acid letter indicates that it is $^{13}C^{\alpha}$-labeled. The "Aib" in the Boc peptides indicates an α-aminoisobutyric acid residue. By using different crystallization solvents (methanol/water[17] or DMSO/2-propanol[18]), the Boc-VAL-Aib-VAL-OMe peptides were crystallized in two different conformations.

NMR Spectroscopy. ^{13}C NMR spectra of both Boc-V*AL-Aib-*VAL-OMe conformers and the Boc-VA*L-Aib-VAL-OMe/MeOH−water peptides were obtained at 7.07 T (corresponding to a ^{13}C Larmor frequency of 75.74 MHz) on a home-built spectrometer based on a Tecmag (Houston, Texas) pulse programmer. A Chemagnetics (Fort Collins, CO) 4-mm MAS probe was used for these experiments. Spinning speeds were controlled to ±1 Hz using a home-built spinning-speed controller. The CP contact time was 2.5 ms, the ^{1}H decoupling field strength was 108 kHz, and the recycle delay was 1.5 s. Spectra of the Boc-VA*L-Aib-VAL-OMe/DMSO−2-propanol peptide, as well as both LLVY-OMe peptide ^{13}C NMR spectra, were obtained at 11.72 T (corresponding to a ^{13}C Larmor frequency of 125.75 MHz) using a Varian/Chemagnetics (Fort Collins, CO) Infinity spectrometer with a 4-mm MAS probe. Spinning speeds were controlled to within ±3 Hz using a Chemagnetics spinning-speed controller. The CP contact time was 2.0 ms, the ^{1}H decoupling field strength was 104 kHz, and the recycle delay was 2 s. The experimental spectra were taken at a range of sample-spinning speeds and fitted by using the Herzfeld−Berger method.[19] An average of the CSA values derived from each spinning speed was used to compare with the theoretically calculated values. Isotropic shift values were measured relative to the carbonyl carbon of glycine in a reference sample, taken as 176.04 ppm downfield from tetramethylsilane (TMS; IUPAC δ-scale).

Computational Aspects. C^{α} shieldings for alanine, valine, and leucine were evaluated by using Hartree−Fock theory and the gauge-including atomic orbitals[20,21] (GIAO) approach. Full Ramachandran chemical shielding surfaces were calculated for leucine in the three most probable conformers found in rotamer libraries:[22,23] $\chi_1 = -60°$, $\chi_2 = 180°$ (**mt**, 59% of rotamer library); $\chi_1 = 180°$, $\chi_2 = 60°$ (**tp**, 29%); and $\chi_1 = 180°$, $\chi_2 = 180°$ (**tt**, 2%). Here **t** = trans, **p** = +60°, and **m** = −60° torsion angles, following Lovell et al.,[23] and for valine in the three most probable χ_1 conformers: $\chi_1 = 180°$ (**t**, 73% of rotamer library); $\chi_1 = -60°$ (**m**, 20%); and $\chi_1 = +60°$ (**p**, 6%). The methods used to compute these shielding surfaces have been described previously.[10] Calculations used a series of *N*-formyl-L-amino acid amide fragments, which are energy-minimized by using an AMBER[24,25] force field in the Discover module imbedded in Insight II (Molecular Simulations, Inc., San Diego, CA). The energy-minimized structures were then used as input structures for evaluation of the chemical shielding surfaces using Gaussian-98.[26] A locally dense basis set approach[27] was employed using a 6-311++G(2d,2p)/6-31G scheme, with the larger basis placed on C^{α} and its neighboring atoms, as depicted in the following diagram for the leucine fragment:

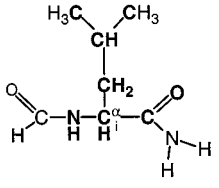

(11) Hong, M. *J. Am. Chem. Soc.* **2000**, *122*, 3762−3770.
(12) Tjandra, N.; Bax, A. *J. Am. Chem. Soc.* **1997**, *119*, 9576−9577.
(13) Walling, A. E.; Pargas, R. E.; de Dios, A. C. *J. Phys. Chem. A* **1997**, *101*, 7299−7303.
(14) Szabo, C. M.; Sanders, L. K.; Arnold, W.; Grimley, J. S.; Godbout, N.; McMahon, M. T.; Moreno, B.; Oldfield, E. In *Modeling NMR Chemical Shifts: Gaining Insights into Structure and Environment*; Facelli, J. C., deDios, A. C., Eds.; ACS Symposium Series 732, 1999; pp 40−62.
(15) Sun H.; Sanders, L. K.; Oldfield, E. Unpublished results.
(16) Precigoux, G.; Courseille, C.; Geoffre, S.; Leroy, F. *J. Am. Chem. Soc.* **1987**, *109*, 7463−7465.
(17) Karle, I. L.; Flippen-Anderson, J. L.; Uma, K.; Balaram, P. *Proteins: Struct., Funct., Genet.* **1990**, *7*, 62−73.
(18) Karle, I. L.; Flippen-Anderson, J. L.; Uma, K.; Balaram, P. *Biopolymers* **1993**, *33*, 827−837.
(19) Herzfeld, J.; Berger. A. E. *J. Chem. Phys.* **1980**, *73*, 6021−6030.
(20) London, F. *J. Phys. Radium* **1937**, *8*, 397−409.
(21) Ditchfield, R. *J. Chem. Phys.* **1972**, *56*, 5688−5691.
(22) Ponder, J. W.; Richards, F. M. *J. Mol. Biol.* **1987**, *193*, 775−791.
(23) Lovell, S. C.; Word, J. M.; Richardson, J. S.; Richardson, D. C. *Proteins: Struct., Funct., Genet.* **2000**, *40*, 389−408.
(24) Weiner, S. J.; Kollman, P. A.; Case, D. A.; Singh, U. C.; Ghio, C.; Alagona, G.; Profeta, S. Jr.; Weiner, P. *J. Am. Chem. Soc.* **1984**, *106*, 765−784.
(25) Weiner, S. J.; Kollman, P. A.; Nguyen, D. T.; Case, D. A. *J. Comput. Chem.* **1986**, *7*, 230−252.

Table 1. Experimentally Measured $^{13}C^{\alpha}$ Chemical Shift Tensor Information for Ala-, Val-, and Leu-containing Peptides

res.	compound	δ_{11} (ppm)	δ_{22} (ppm)	δ_{33} (ppm)	$\delta_{11}-\delta_{33}$ (ppm)
Ala	**1** Boc-V*AL-Aib-VAL-OMe[a]	73.8	52.0	32.5	41.3
	2 Boc-V*AL-Aib-VAL-OMe[b]	73.0	51.3	32.6	40.4
	3 G*AV[c]	76.9	55.4	25.5	51.4
	4 A*AA[c]	70.2	54.9	23.6	46.6
	5 A*AA • hemihydrate[c]	71.0	55.8	24.0	47.0
Val	**6** Boc-VAL-Aib-*VAL-OMe[a]	79.1	62.8	38.2	40.9
	7 Boc-VAL-Aib-*VAL-OMe[b]	78.7	61.8	38.0	40.7
	8 LL*VY−OMe	79.3	57.1	39.8	39.5
Leu	**9** Boc-VA*L-Aib-VAL-OMe[a]	71.4	54.8	40.2	31.2
	10 Boc-VA*L-Aib-VAL-OMe[b]	71.5	57.7	36.1	35.4
	11 L*LVY−OMe	71.6	50.9	31.3	40.3

[a] Crystallized from MeOH−H_2O. [b] Crystallized from DMSO−2-propanol. [c] Experimental values from ref 9.

These shielding surfaces along with the previously reported alanine surfaces[10] can be found at http://feh.scs.uiuc.edu.

To obtain the tensor orientations necessary for conversion of solid-state δ_{ii} to solution $\Delta\sigma^*_{exp}$ values, individual calculations were performed for the 11 labeled sites in the polypeptides of interest, shown in Table 1. These calculations utilized the energy minimized amino acid model compound with the ϕ,ψ torsion angles set to corresponding crystallographic values, while the χ_1/χ_2 torsion angles were set to the nearest staggered energy minimum value ($\pm 60°$, 180°).

Calculations were performed on Silicon Graphics Origin 200 (Mountain View, CA) computers in this laboratory and on the Silicon Graphics Origin 2000 and HP-Convex Exemplar SP-2000 (Hewlett-Packard Company, Palo Alto, CA) computers located in the National Center for Supercomputing Applications (NCSA) in Urbana, IL.

Results and Discussion

We first investigated the $^{13}C^{\alpha}$ shift tensor elements in the following peptides (Table 1): Boc-V*AL-Aib-*VAL-OMe (MeOH/water) (**1,6**), Boc-V*AL-Aib-*VAL-OMe (DMSO/2-propanol) (**2,7**), G*AV (**3**), A*AA (**4**) A*AA-hemihydrate (**5**), LL*VY-OMe (**8**), Boc-VA*L-Aib-VAL-OMe (MeOH/water) (**9**), Boc-VA*L-Aib-VAL-OMe (DMSO/2-propanol) (**10**), and L*LVY-OMe (**11**), where the asterisk preceding a letter indicates the presence of a $^{13}C^{\alpha}$-labeled residue. We used magic-angle sample-spinning NMR to obtain spectra at a series of spinning speeds, and then used the Herzfeld−Berger[19] method to deduce the principal elements of the $^{13}C^{\alpha}$ shift tensor: δ_{11}, δ_{22}, and δ_{33}. A spectrum of Boc-VA*L-Aib-VAL-OMe (**9**) obtained with high-power proton-decoupling is shown in Figure 1B, together with its computer simulation (Figure 1A) and the difference spectrum, Figure 1C. The experimentally determined shift tensor elements for the eight $^{13}C^{\alpha}$-labeled sites in the new compounds, together with results for the three alanine-containing peptides reported previously,[9] are shown in Table 1.

To evaluate the theoretical shieldings, we used the alanine-shielding surfaces reported previously,[10] together with the new

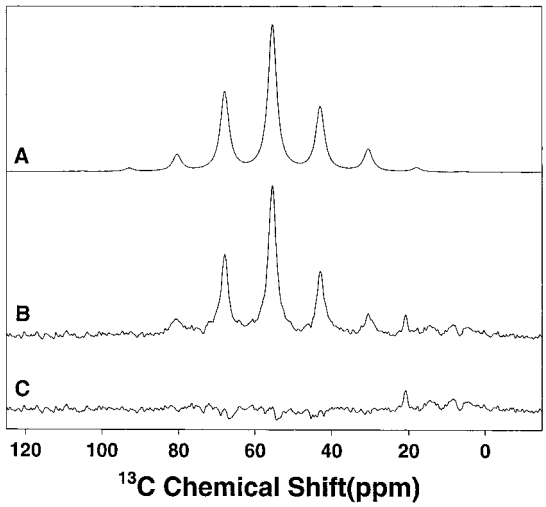

Figure 1. CP-MAS NMR results for $^{13}C^{\alpha}$-labeled Boc-VA*L-Aib-VAL-OMe (**9**). (A), Computer simulation of experimental spectrum, (B). The MAS spinning rate was 935 Hz, and the spectrum in (B) was referenced to $^{13}C^{o}$ in glycine taken to be at 176.04 ppm downfield from TMS. (C) Difference between (A) and (B).

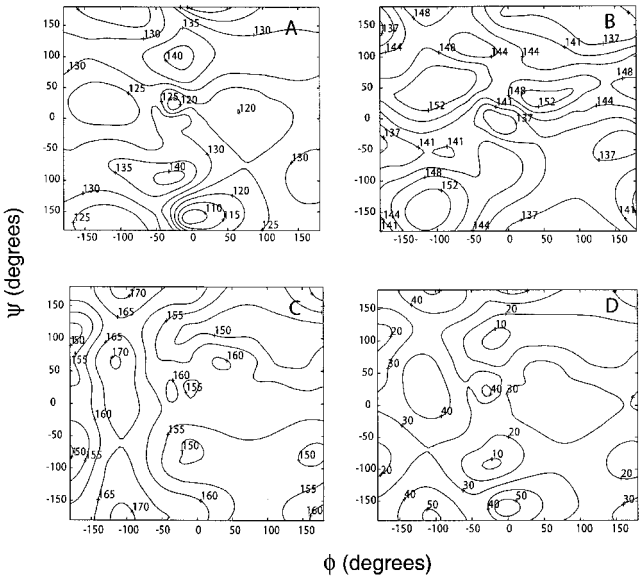

Figure 2. Computed shielding surfaces for $^{13}C^{\alpha}$ in *N*-formyl leucine amide ($\chi_1 = -60°$, $\chi_2 = 180°$, **mt**, 59% of the protein database), computed by using a Hartree−Fock method with gauge-including atomic oribtals and a locally dense basis set: (A) σ_{11}; (B) σ_{22}; (C) σ_{33}; and (D) $\sigma_{33} - \sigma_{11}$.

leucine and valine surfaces. The individual shielding tensor surfaces $\sigma_{ii}\, f(\phi,\psi)$ and the shielding tensor span surface $\Omega f(\phi,\psi)$ for the three most probable conformations of leucine are shown in Figures 2−4. In Table 2, we show the crystallographic ϕ, ψ and χ values and computed shielding tensor values for the 11 C^{α}-labeled sites. For alanine, we predicted 15 shielding tensor elements from the experimental ϕ,ψ results for **1**−**5**, and these are shown in Table 2 and Figure 5A. From Figure 5A, we deduce the following relationship between the theoretical shielding tensor elements (σ_{ii}) and the experimental shift tensor elements (δ_{ii}):

$$\sigma_{ii}^{A} = -0.72\delta_{ii}^{A} + 184.6 \quad (R^2 = 0.97) \qquad (1)$$

where σ_{ii}^{A} is the theoretical shielding tensor element for $^{13}C^{\alpha}$ in an alanine peptide (in ppm from the bare nucleus) and δ_{ii}^{A} is

(26) Frisch, M. J.; Trucks, G. W.; Schlegel, H. B.; Scuseria, G. E.; Robb, M. A.; Cheeseman, J. R.; Zakrzewski, V. G.; Montgomery, J. A., Jr.; Stratmann, R. E.; Burant, J. C.; Dapprich, S.; Millam, J. M.; Daniels, A. D.; Kudin, K. N.; Strain, M. C.; Farkas, O.; Tomasi, J.; Barone, V.; Cossi, M.; Cammi, R.; Mennucci, B.; Pomelli, C.; Adamo, C.; Clifford, S.; Ochterski, J.; Petersson, G. A.; Ayala, P. Y. Cui, Q.; Morokuma, K.; Malick, D. K.; Rabuck, A. D.; Raghavachari, K.; Foresman, J. B.; Cioslowski, J.; Ortiz, J. V.; Baboul, A. G.; Stefanov, B. B.; Liu, G.; Liashenko, A.; Piskorz, P.; Komaromi, I.; Gomperts, R.; Martin, R. L.; Fox, D. J.; Keith, T.; Al-Laham, M. A.; Peng, C. Y.; Nanayakkara, A.; Gonzalez, C.; Challacombe, M.; Gill, P. M. W.; Johnson, B.; Chen, W.; Wong, M. W.; Andres, J. L.; Gonzalez, C.; Head-Gordon, M.; Replogle, E. S.; Pople, J. A. *Gaussian 98*, Revision A.7; Gaussian, Inc.: Pittsburgh, PA, 1998.

(27) Chestnut, D. B.; Moore, K. D., *J. Comput. Chem*. **1989**, *10*, 648−659.

Table 2. X-ray ϕ, ψ, χ_1, χ_2 Values[a] and Computed $^{13}C^{\alpha}$ Shielding Tensor Information[b]

res	compound	Φ (deg)	Ψ (deg)	χ_1 (deg)	χ_2 (deg)	σ_{11} (ppm)	σ_{22} (ppm)	σ_{33} (ppm)	$\Omega = \sigma_{33}$-σ_{11} (ppm)	$\Delta\sigma$*theory (ppm)	$\Delta\sigma$*exp (ppm)
Ala	**1** Boc-V*Al-Aib-VAL-OMe[b]	−65.4	−44.5			129.30	147.0	162.3	33.0	2.5	1.5
		−61.0	−44.4								
	2 Boc-V*Al-Aib-VAL-OMe[c]	−76.0	−44.0			130.4	145.0	165.2	34.8	7.6	4.4
	3 G*AV	−68.7	−38.1			129.5	146.2	164.5	35.0	6.6	9.2
	4 A*AA	−143.4	160.2			132.9	148.2	165.9	33.0	23.0	28.5
		−164.1	149.0								
	5 A*AA • hemihydrate	−145.7	145.5			133.8	149.0	164.7	30.9	22.0	29.1
		−156.2	149.9								
Val	**6** Boc-VAL-Aib-*VAL-OMe[c]	−90.9	1.5	−58.5		121.8	133.6	159.3	37.5	25.0	27.5
		−87.2	−10.8	−61.0							
	7 Boc-VAL-Aib-*VAL-OMe[d]	−109.0	17.0	−56.0		116.7	139.7	164.0	47.3	32.0	28.3
	8 LL*VY−OMe	−123.9	119.7	−179.9		118.9	143.8	158.5	39.6	24.4	29.4
Leu	**9** Boc-VA*L-Aib-VAL-OMe[e]	−68.2	−38.4	−176.2	57.3	130.0	142.2	158.5	28.5	11.0	9.1
		−70.8	−35.2	−168.9	61.0						
	10 Boc-VA*L-Aib-VAL-OMe[d]	−62.0	−29.0	−60	180[e]	128.4	141.6	160.4	32.0	7.8	8.6
	11 L*LVY-OMe	−129.4	123.7	−60	180[e]	130.5	146.7	161.3	30.8	26.0	30.1

[a] From refs 9,16−18. [b] Theoretical tensor values determined from Ramachandran shielding surfaces. [c] Crystallized from MeOH−H_2O. [d] Crystallized from DMSO−2-propanol. [e] From molecular mechanics results.

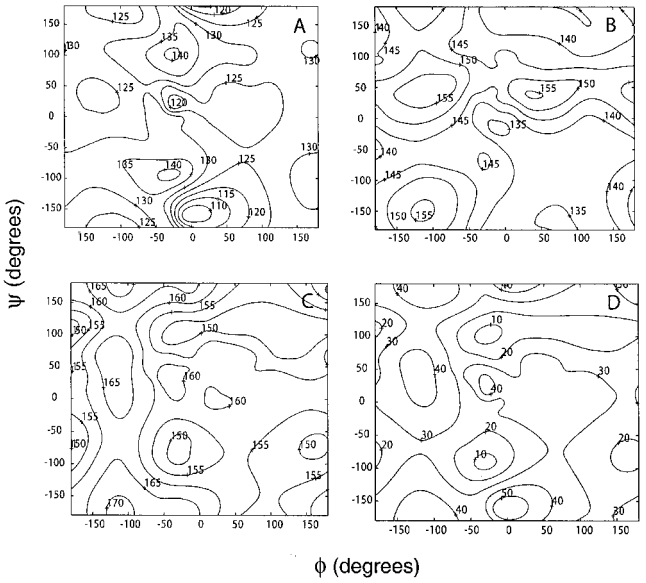

Figure 3. Computed shielding surfaces for $^{13}C^{\alpha}$ in *N*-formyl leucine amide ($\chi_1 = 180°$, $\chi_2 = 60°$, **tp**, 29% of the protein database). Computed by using a Hartree−Fock method with gauge-including atomic orbitals and a locally dense basis set: (A) σ_{11}; (B) σ_{22}; (C) σ_{33}; and (D) $\sigma_{33} - \sigma_{11}$.

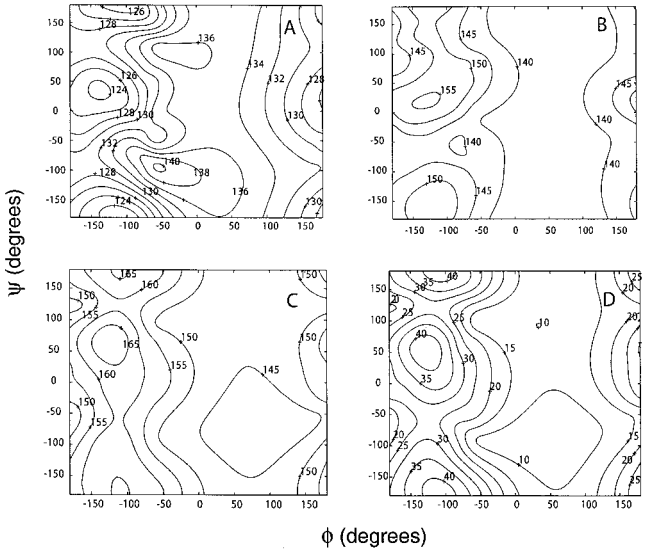

Figure 4. Computed shielding surfaces for $^{13}C^{\alpha}$ in *N*-formyl leucine amide ($\chi_1 = 180°$, $\chi_2 = 180°$, **tt**, 2% of the protein database). Computed by using a Hartree−Fock method with gauge-including atomic orbitals and a locally dense basis set: (A) σ_{11}; (B) σ_{22}; (C) σ_{33}; and (D) $\sigma_{33} - \sigma_{11}$.

the experimental chemical shift tensor element (in ppm from tetramethylsilane, TMS). Two shielding surfaces, with $\chi_1 = -60°$ and $\chi_1 = 180°$, were then used to evaluate the nine valine $^{13}C^{\alpha}$ shielding tensor elements shown in Tables 1 and 2, and these results are plotted in Figure 5B. From this we deduce the relation:

$$\sigma_{ii}^{V} = -1.03\delta_{ii}^{V} + 200.8 \quad (R^2 = 0.99) \qquad (2)$$

Clearly, in both alanine and valine, the R^2 values are excellent, with the rms deviations from the fitted line being on average ~2.0 ppm, indicating that the theoretical predictions correlate well with those determined experimentally.

For leucine, we computed the three major shielding surfaces:[23,24] $\chi_1 = -60°$, $\chi_2 = 180°$ (**mt**, 59% of the protein database); $\chi_1 = 180°$, $\chi_2 = 60°$ (**tp**, 29% of the database) and $\chi_1 = 180°$, $\chi_2 = 180°$ (**tt**, 2% of the protein database). Unlike the situation found with the two valine-containing peptides, the X-ray crystallographic results for leucine peptides showed side chain disorder in two out of three three peptides investigated, and we did not obtain crystals suitable for a reanalysis of this question. Fortunately, however, the shielding surfaces for the major conformations, Figures 2−4, are rather similar, and we find good correlations between all nine experimental shifts and their corresponding computed shielding tensor elements when using either the most probable **mt** or **tp** surfaces. That is, the $^{13}C^{\alpha}$ shielding tensor is primarily sensitive to ϕ,ψ changes, not to differences in χ_1 and χ_2. In **9**, only the **tp** conformers are present (two molecules per unit cell) but in **10** there are four conformers (including the most populated **mt** and **tp** species) and in **11** there are two. Fortunately, however, as noted above and as shown in Figures 2−4, the $^{13}C^{\alpha}$ shielding tensors are relatively insensitive to χ_1/χ_2 for this amino acid (unlike the situation with, e.g., isoleucine), and use of either of the most populated (**mt**, **tp**) surfaces produces very similar $^{13}C^{\alpha}$ shielding tensor results. For example, using the **mt** ($\chi_1 = -60°$, $\chi_2 = 180°$) surface we obtain a slope = −0.87, an intercept = 191.5 ppm and an R^2 value = 0.97, and a rmsd from the fitted line of 2.4 ppm. For the **tp** surface ($\chi_1 = 180°$, $\chi_2 = 60°$) we obtain a slope = −0.82,

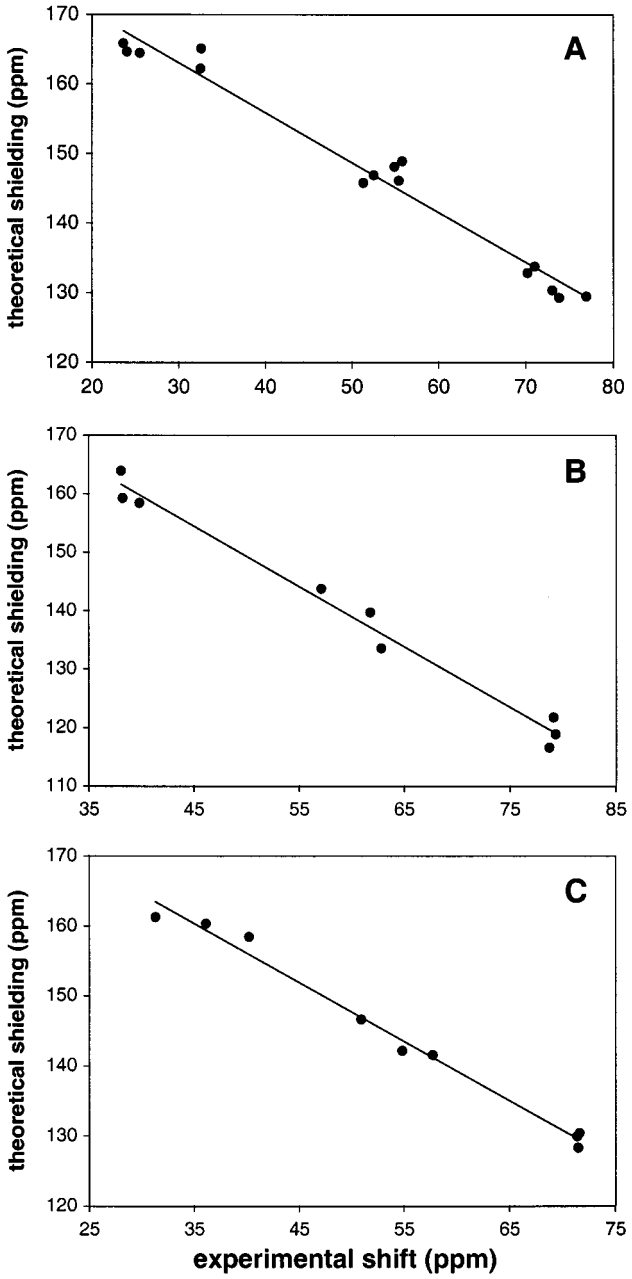

Figure 5. Graph showing theoretical $^{13}C^{\alpha}$ chemical-shielding tensor elements for alanine (A), valine (B), and leucine (C) peptides plotted versus the experimentally determined chemical shift tensors. For (A): slope = −0.72, *y*-intercept = 184.6 ppm, R^2 = 0.97, and rmsd = 2.4 ppm. (B): slope = −1.03, *y*-intercept = 200.8 ppm, R^2 = 0.98, and rmsd = 2.5 ppm. For (C): slope = −0.84, *y*-intercept = 189.8 ppm, R^2 = 0.99, and rmsd = 1.5 ppm.

an intercept = 188.9 ppm, an R^2 value = 0.98, and an rmsd = 1.7 ppm.

However, it is of course most appropriate to try to use the actual or most probable conformers. For **9**, we used the **tp** surface to generate the theoretical shielding results shown in Table 2, since there is only a single conformer in the crystal. For **11**, there are two conformers present; however, one of these appeared to have a bad steric contact with the tyrosine ring in the peptide, and on molecular mechanics geometry optimization adopted the **mt** conformation, which was used to generate the shielding results given in Table 2. Similarly, **10** was also subjected to molecular mechanics optimization and yielded **mt** as the preferred conformation, again resulting in the shielding

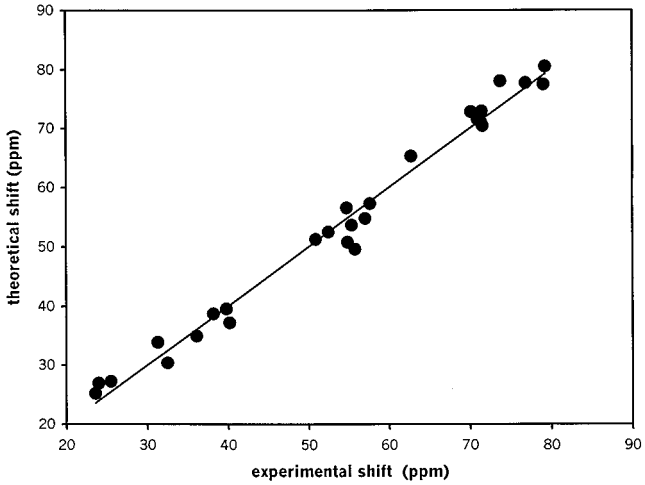

Figure 6. Theory versus experiment comparison of chemical shift tensor elements for Ala, Val, and Leu peptides. The theoretical chemical shifts are corrected by use of eqs 1−3. Slope = 1.00, *y*-intercept = −0.12 ppm, R^2 = 0.99, and rmsd = 2.7 ppm.

results shown in Table 2. A graph of the experimental shift versus theoretical shielding tensor elements is shown in Figure 5C and can be fitted by:

$$\sigma_{ii}^{L} = -0.84\,\delta_{ii}^{L} + 189.8 \quad (R^2 = 0.99) \qquad (3)$$

with an rms error of 1.5 ppm.

When considering all 33 shift tensor element results, we conclude that the quantum chemical shielding calculations generate good correlations between the experimental shift and theoretical shielding tensor values. However, while the R^2 values are in all cases very good (R^2 values of ∼0.99, on average), there are clearly small systematic errors in the slopes, which range from −0.72 to −1.03 (versus the ideal value of −1.00). This effect has been discussed previously,[2] and we have proposed that since the R^2 values are so good, it is appropriate to simply use regression curve slopes and intercepts to scale the quantum chemical results to arrive at accurate predicted shift values.

Using the appropriate scalings from the regression curves (eqs 1−3), we obtained the experimental shift versus theoretical shift tensor element results shown in Figure 6, where there is clearly very good agreement for all 33 $^{13}C^{\alpha}$ shift tensor elements in alanine, valine, and leucine fragments. Also of interest from these results, and those shown in Table 2, is the observation that while the expected isotropic shift/shielding difference between helical and sheet residues is seen in each case, that is, the sheets are ∼3−4 ppm more shielded than are helical $^{13}C^{\alpha}$ residues, there is no evidence for any "narrow" helical $^{13}C^{\alpha}$ CSAs or Ωs.

The reasons for the lack of large helix-sheet CSA differences are as follows. First, in the case of alanine, we have already demonstrated both experimentally and theoretically that there are no major helix/sheet tensor anisotropy differences seen.[9,10] Second, in the case of the three valine residues investigated, **6** is a $\chi_1 = -60°$ distorted helix ($\phi = -87°$, $\psi = -11°$, molecule 1; $\phi = -91°$, $\psi = 2°$, molecule 2). The average Ω for these two species (from the shielding surfaces) is 38.8 ppm. The second valine species, **7**, is a $\chi_1 = -60°$ distorted sheet ($\phi = -109°$, $\psi = 17°$). The Ω for **7** from the shielding surfaces is 47.3 ppm. The final valine species, **8**, is a $\chi_1 = 180°$ sheet ($\phi = -124°$, $\psi = 120°$). The Ω for **8** from the shielding surfaces is 39.6 ppm, in general accord with the 37.4 previously reported

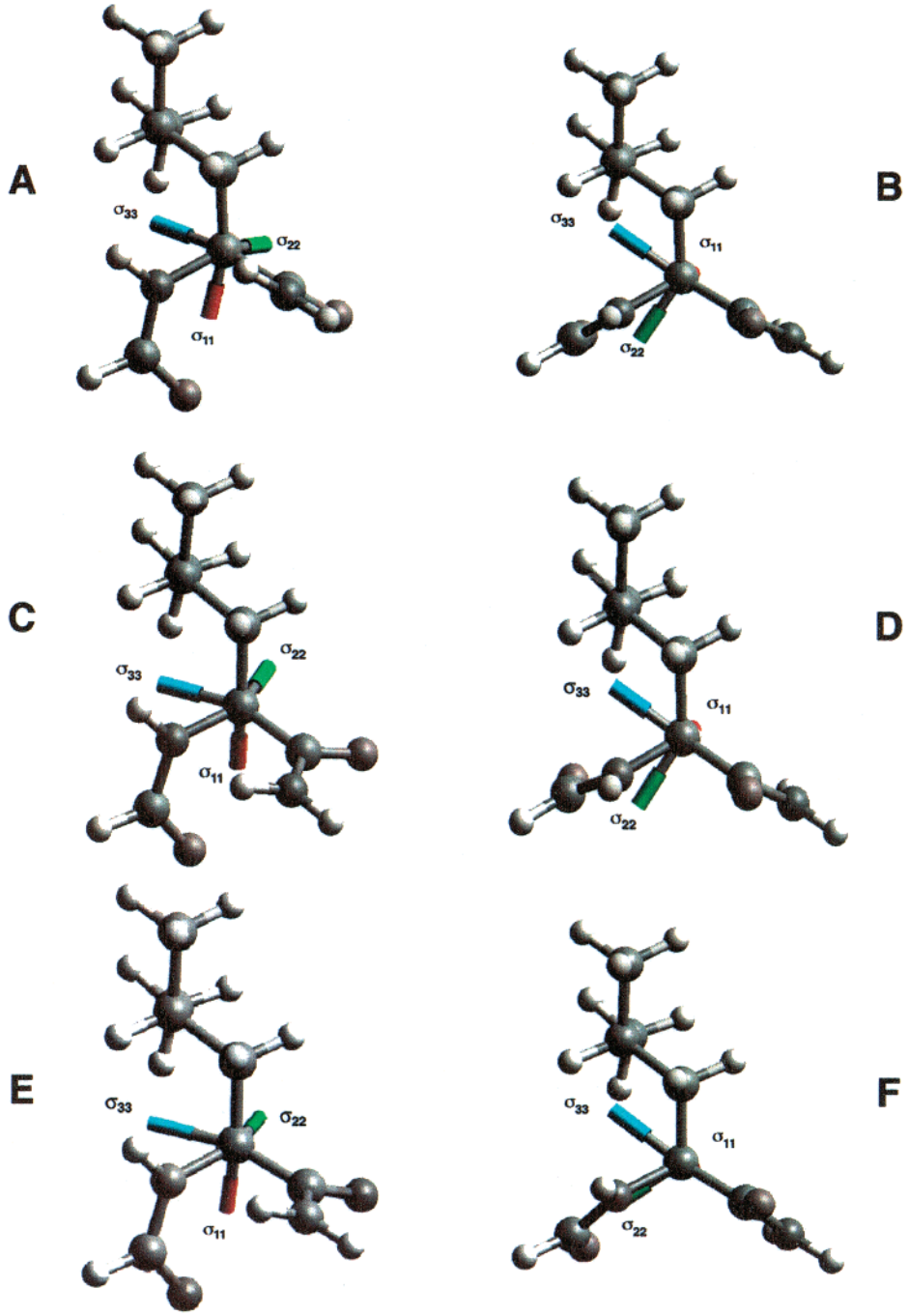

Figure 7. $^{13}C^{\alpha}$ shielding tensor orientations for fragments investigated. (A) "Ideal" leucine helix geometry ($\phi = -60°$, $\psi = -60°$); $\Delta\sigma = 28.1$ ppm, $\Delta\sigma^* = 1.34$ ppm; (B) "Ideal" sheet geometry ($\phi = -120°$, $\psi = 120°$); $\Delta\sigma = 34.8$ ppm, $\Delta\sigma^* = 26.8$ ppm; (C) Compound **10** ($\phi = -62°$, $\psi = -29°$); $\Delta\sigma = 32.0$ ppm, $\Delta\sigma^* = 7.8$ ppm; (D) Compound **11** ($\phi = -129°$, $\psi = 124°$); $\Delta\sigma = 30.8$ ppm, $\Delta\sigma^* = 26.0$ ppm; (E) Ubiquitin Leu 56 (($\phi = -61°$, $\psi = -36°$); $\Delta\sigma = 32.0$ ppm, $\Delta\sigma^* = 6.5$ ppm and (F) Ubiquitin Leu 69 ($\phi = -107°$, $\psi = 116°$); $\Delta\sigma = 34.1$ ppm, $\Delta\sigma^* = 25.7$ ppm.

for the $\phi = -120°$, $\psi = 120°$ $\chi_1 = 180°$ sheet.[10] In the case of the three leucine species, **9**−**11**, **9** and **10** have helical ϕ,ψ values while **11** has sheet values (Table 2). However, as demonstrated by both experiment (Table 1) and theory (Table 2) there are in fact no major differences in Ω between helical and sheet geometries. In sharp contrast, helical and sheet leucine $\Delta\sigma$*s determined via solution NMR do vary widely with conformation. The reason for these differences must therefore reside in the definition of the "CSA".

According to Jameson,[28] Ω is the difference between the most-shielded (σ_{33}) and the least-shielded tensor component (σ_{11}), corresponding to the width of the resonance powder pattern in ppm, $\Omega \equiv (\sigma_{33} - \sigma_{11})$, where $\sigma_{33} \geq \sigma_{22} \geq \sigma_{11}$ and σ is the chemical *shielding*, and $\Omega \simeq (\delta_{11} - \delta_{33})$, where δ is the chemical *shift*.

Previously, we used Ω to describe shielding tensor differences between helices and sheets, which is used in CSA-based dephasing experiments,[11] where the dephasing observed is a function of Ω . Relaxation-based measurement of the CSA in solution NMR is, however, sensitive to different components of the CSA. Here, a CSA or $\Delta\sigma^*$ has been defined as $\Delta\sigma^* = \sigma_{orth} - \sigma_{par}$, where σ_{par} is the shielding parallel to the $C^{\alpha}-H^{\alpha}$ bond vector and σ_{orth} is the average shielding orthogonal to the

(28) Jameson, C. J. *Solid State NMR* **1998**, *11*, 265−268.

$C^{\alpha}-H^{\alpha}$ bond vector. However, if we know the angles between σ_{ii} and the $C^{\alpha}-H^{\alpha}$ bond vector, the shielding tensor can be projected onto this axis by using the following rotation:

$$\sigma_{par} = [d_1 \;\; d_2 \;\; d_3]\begin{bmatrix}\sigma_{11} & 0 & 0\\ 0 & \sigma_{22} & 0\\ 0 & 0 & \sigma_{33}\end{bmatrix}\begin{bmatrix}d_1\\ d_2\\ d_3\end{bmatrix} \quad (4)$$

where σ_{ii} are the shielding tensor elements in the principal axis system and d_i are the direction cosines of the $C^{\alpha}-H^{\alpha}$ bond with respect to the principal axes. When combined with eq 5:[12]

$$\Delta\sigma^* = \sigma_{orth} - \sigma_{par} = 1.5^* \quad (\sigma_{iso} - \sigma_{par}) \quad (5)$$

$\Delta\sigma^*$ can therefore in principle be calculated from σ_{11}, σ_{22}, σ_{33}, and the direction cosines. Unfortunately, in simple solid-state MAS NMR experiments, only the magnitudes of the shift tensor elements are obtained, so that the solid-state NMR Ω information cannot immediately be transformed to the solution NMR $\Delta\sigma^*_{exp}$ by means of eqs 4 and 5. However, it seems reasonable to utilize the tensor orientations (d_1, d_2, d_3) we obtain from ab initio calculations to effect this transformation, since in previous work we have shown excellent agreement between single-crystal shielding tensor results and theoretical shielding tensor results in the amino acid threonine.[29] Therefore, by using eq 6, $\Delta\sigma^*_{exp}$ for the 11 labeled sites can be computed from the solid-state NMR δ_{ii}^{exp} results as:

$$\Delta\sigma^*_{exp} = -1.5 \times \left(\delta_{iso}{}^{exp} - [d_1 d_2 d_3]\begin{bmatrix}\delta_{11}{}^{exp} & 0 & 0\\ 0 & \delta_{22}{}^{exp} & 0\\ 0 & 0 & \delta_{33}{}^{exp}\end{bmatrix}\begin{bmatrix}d_1\\ d_2\\ d_3\end{bmatrix} \right) \quad (6)$$

Clearly, from eq 6 above, the orientation of the principal axis can significantly affect the values of $\Delta\sigma^*$. As may be seen in Figure 7, the computed C^{α} shielding tensor orientations in leucine do vary dramatically with ϕ,ψ, and consequently the shieldings along the $C^{\alpha}-H^{\alpha}$ bond axis also vary considerably. This of course explains why ab initio quantum chemical calculations of protein solution NMR $\Delta\sigma^* = \sigma_{orth} - \sigma_{par}$ values using an alanine model are in generally good agreement with experiment,[4,14] even though the $\Delta\sigma = \Omega = \sigma_{33} - \sigma_{11}$ values are relatively insensitive to ϕ,ψ, both experimentally[9] and theoretically.[9,10] That is, the alanine tensor orientation changes overwhelmingly dominate the helical/sheet $\Delta\sigma^*$ changes, because alanine is not a β-branched amino acid and is therefore a good model for the great majority of amino acids.

To demonstrate this effect more clearly, we show in Figure 8 the $\Delta\sigma^*_{exp}$ (eq 6) and purely theoretical $\Delta\sigma^*$ values (Table 2) for the 11 labeled sites investigated, together with solution NMR results for Ala, Val, and Leu in the protein ubiquitin. The solid state $\Delta\sigma^*_{exp}$ values were obtained by combining the experimental δ_{ii} with the theoretical direction cosines, as shown in eq 6. The ubiquitin solution $\Delta\sigma^*_{exp}$ values are those reported by Tjandra and Bax.[12] The $\Delta\sigma^*$ (theoretical) values were read from the theoretical $\Delta\sigma^*$ surfaces. When cast in terms of solution $\Delta\sigma^*$ values, the solid-state results are clearly indistinguishable from the solution NMR results. Thus, although $\Delta\sigma = \Omega$ for leucine is essentially independent of whether $^{13}C^{\alpha}$ is in a helical or sheet conformation (Ω is ~37 ppm on average from experiment, ~30 ppm from calculation), $\Delta\sigma^*$ (solution) varies from ~5 to 38 ppm (from ref 12), as does the solid-state derived $\Delta\sigma^*$ (~10−30 ppm, Table 2).

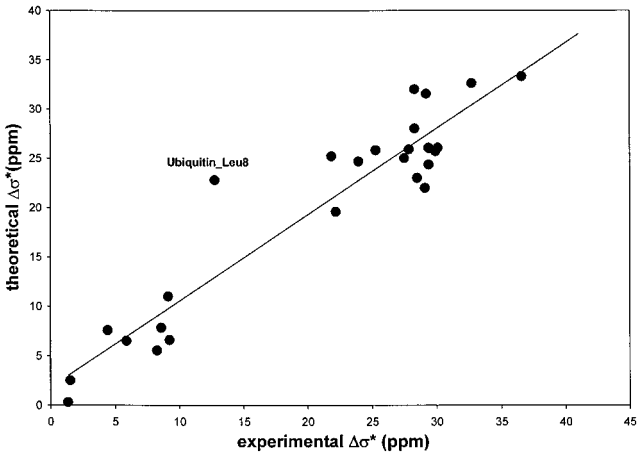

Figure 8. Theory versus experiment comparison of the C^{α} solution CSA ($\Delta\sigma^* = \sigma_{orth} - \sigma_{par}$) for Ala, Val, Leu in ubiquitin and nine peptides. Slope = 0.87, *y*-intercept = 1.8 ppm, $R^2 = 0.90$, and rmsd = 3.4 ppm. The outlier in ubiquitin (Leu 8, in a loop) was included in the correlation.

These results have important implications for investigations of Ω in other amino acids in peptides or proteins, in particular for their use in spectral editing or in deriving structural information. For example, in recent solid-state NMR studies of ubiquitin,[11] it has been shown that there are large differences in signal dephasing which depend on Ω, with β-sheet $^{13}C^{\alpha}$ signals decaying first. In one spectral region, Gln-40, Glu-41, and Phe-4 all decayed rapidly, consistent with a large Ω (all are non-β-branched residues). Similarly, in another spectral region, Val-70 (sheet, $\chi_1 = 180°$) and Ileu-13 (sheet, $\chi_1 = 126°$) also decayed rapidly (sheet Ωs, even for β-branched amino acids, are large), while Ileu-23 (helix), Val-26 (helix), and Ileu-30 (helix) all remained prominent, consistent with small Ωs. The helical residues Lys-33, Glu-34, and Tyr-59 were apparently exceptions; however, this may be attributable to the fact that all three amino acids have similarly large helix, sheet tensor spans, since they are not β-branched.[15]

Conclusions

The results we have presented above are of interest for a number of reasons. Not only have we obtained experimental $^{13}C^{\alpha}$ shielding tensor results for unbranched (alanine, leucine) and β-branched (valine) amino acids in peptides using magic-angle sample spinning techniques, but we also find good correlations between these experimental shielding results and those computed theoretically. Our results with the unbranched amino acids alanine and leucine show very similar $^{13}C^{\alpha}$ tensor magnitudes for helical and sheet conformations, but with different tensor orientations. This is to be compared with previous results with valine, isoleucine, and threonine, in which small $^{13}C^{\alpha}$ tensor spans (Ω) were predicted for helical (but not sheet) residues for the most popular conformations. The lack of large variations in Ω for non-β-branched amino acids may be a general one and has implications for structural studies or solid-state spectral editing experiments based on Ω. Finally, we were able to clarify differences between the solution-state derived $\Delta\sigma^*$ and the solid-state definition of the CSA. Our results show that there is good agreement between experimental and theoretical $\Delta\sigma^*$ values for alanine, valine, and leucine residues in ubiquitin (solution NMR) and in a series of peptides (solid-state MAS NMR σ_{ii} determination, ab initio tensor

(29) De Dios, A. C.; Laws, D. D.; Oldfield, E. *J. Am. Chem. Soc.* **1994**, *116*, 7784−7786.

orientation). The broad range of $\Delta\sigma^*$ but essentially constant Ω values are well reproduced in the calculations. The range in $\Delta\sigma^*$ in solution NMR experiments is overwhelmingly dominated by changes in the $^{13}C^{\alpha}$ tensor orientation with ϕ,ψ. An exciting prospect of the sensitivity of the CSA tensor and its orientation to ϕ and ψ is that this may allow the CSA to be used as an effective structure refinement tool. Advances in cross-correlated relaxation measurement in solution have shown that both the shift tensor and its orientation can be determined in proteins,[30] and further work utilizing the results presented here is currently underway.[31]

Acknowledgment. We thank David King and Haydn Ball for synthesizing the peptides. R.H.H. gratefully acknowledges the National Science Foundation for a predoctoral fellowship. D.D.L. gratefully acknowledges the Howard Hughes Medical Institute for a pre-doctoral fellowship. This work was supported by the Office of Basic Energy Sciences, Materials Sciences Division of the U.S. Department of Energy (Contract No. DE AC03-76SF00098), by the United States Public Health Service (NIH Grants GM-50694 and AG-10770), and by the National Computational Science Alliance (NSF Grant MCB000018N).

JA0115060

(30) Pang, Y.; Zuiderweg, E. R. P. *J. Am. Chem. Soc*. **2000**, *122*, 4841−4842.

(31) Havlin, R. H., Nguyen, T., Walls, J. D. and Wemmer, D. E. Unpublished results.